J Math Imaging Vis (2008) 30: 221–230
DOI 10.1007/s10851-007-0052-3

Perspective Geometry Based Single Image Camera Calibration

N. Avinash · S. Murali

Published online: 20 December 2007

Abstract This paper presents a novel method for 3D camera calibration. Calculation of the focal length and the optical center of the camera are the main objectives of this research work. The proposed technique requires a single image having two vanishing points. A rectangular prism is employed as the calibration target to generate vanishing points. The special arrangement of the calibration object adds more accuracy in finding the intrinsic parameters. Based on the geometry of the perspective distortion of the edges of the prisms from the image, vanishing points are found. There on, fixing up the picture plane followed by fixing up of the station point is carried out based on the relations that are formulated. Experimental results of our method are likened with Zhang's method. Results are tabulated to show the accuracy of the proposed approach.

Keywords Camera calibration · Vanishing points · Horizon line · Picture plane · Focal length · Center of focus

1 Introduction

The purpose of camera calibration is to shew the relationship between 3D world coordinates and their corresponding 2D image coordinates as seen by the camera. The drop from 3-dimensional world to a 2-dimensional image is a projection process in which we lose one dimension. With the help of the relationship established, 3D information can be inferred from the geometric properties of the object. Approaches to camera calibration distinguish two steps in the calibration procedure, viz.

(i) Intrinsic calibration—The determination of the pixel-to-ray mapping with respect to a coordinate system fixed to the camera. i.e., finding the center of focus, focal length etc.
(ii) Extrinsic calibration—The determination of the rotation and translation that link the camera coordinate system to the world coordinate system. i.e., finding the pose of the camera.

The 3D information finds applications like, scene mosaicing and depth estimation etc. Both intrinsic and extrinsic calibration methods have been examined by several researchers. The classical approach [1] that originates from the field of photogrammetry solves the problem by minimizing a non linear error function. Due to slowness and computational burden of this technique, closed-form solutions have been also suggested [2, 3]. However, these methods are based on certain simplification in the camera model, and therefore, they do not provide as good results as non-linear minimization do. There are various methods that use geometric objects whose images have some characteristics that are invariant to the actual position of the object in space and can be used to calibrate some of the camera parameters [4–7]. The use of vanishing points of parallel lines drawn on the faces of a cube is one of those and can be used to obtain the pose of the camera and some of the intrinsic parameters. A variety of methods based on this principle are explored in [4, 8–14]. Willson and Shafer [13] enclose definitions for the center of focus as the center of the field of vision. This is also the optical center of the lens used in the camera for acquiring the image. Zhang's method [18], uses a simple planar pattern for the experimentation and provides

N. Avinash (✉) · S. Murali
Department of Information Science and Engineering,
P.E.T. Research Center, P.E.S. College of Engineering,
Mandya, Karnataka 571401, India
e-mail: wittybot@gmail.com

S. Murali
e-mail: nymurali@yahoo.com

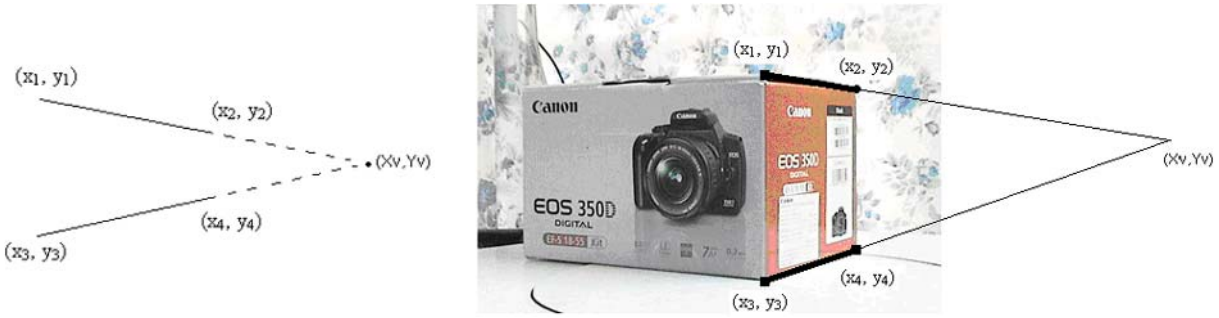

Fig. 1 Depiction of vanishing point in a perspective image

the research community with both easy-to-use and accurate algorithm for obtaining camera parameters. This is the most widely used algorithm with various available libraries [24] like Intel's OpenCV [26] and Matlab Camera Calibration Toolbox [25].

In this paper, we propose a method to estimate the focal length and the center of focus based on the known geometry of the rectangular prism. The rectangular prism is the object we use for our experimentation purpose, and hence we call it as the calibration object. Easily available natural rectangular prisms in general scenes are cartons, boxes and buildings. Although we've used cartons and boxes for our experimentation throughout this object, it was required a checker board pattern (calibration object) for Zhang's method. Hence, we've incorporated patterns of checker board on one face of the box, so that the same image applies for both the experimentations and the results can be compared. That is the box in the image works as calibration object for our method and the checker board pattern acts as calibration object for Zhang's method.

This paper is divided into following sections. The next section introduces the geometrical framework of the formulations made. Ulterior sections, viz. Sects. 3 and 4 explain about the basic setup of the experimentation and followed by calibration algorithm. Section 5 describes the experimental results and concluding remarks are made in Sect. 6. The figures in the results section shows the image sets considered for Zhang's method and also images considered for our method for camera calibration.

2 Geometrical Framework

2.1 Framework for Vanishing Point Detection

The parallel edges of the rectangular prism do not appear parallel in an image due to perspective distortion. The edge of the prism joining points (x_1, y_1), (x_2, y_2) form a line which is actually parallel to the edge formed by joining the points (x_3, y_3) and (x_4, y_4). But in the image it does not seem to be parallel since image is acquired on the principle of pinhole camera. This means image acquisition is based on the perspective projection principle. Therefore in the image as shown in Fig. 1, if these lines are extended, they meet at a point (Xv, Yv) and is called as the Vanishing Point [16]. This is as shown in Fig. 1. If line 1 is the line joining points (x_1, y_1), (x_2, y_2) and line 2 is the line joining the points (x_3, y_3), (x_4, y_4) and m_1, m_2 are the slopes of these lines respectively. Equations for these lines are given by

$$(y - y_1) = m_1(x - x_1) \tag{1}$$

$$(y - y_3) = m_2(x - x_3) \tag{2}$$

These lines are non parallel as told before, and they meet at some point (Xv, Yv) if they are extended on either ends. But, only at the point at which lines intersect, it satisfies both (1) and (2) for the point (Xv, Yv). Hence rearranging these equations after substituting (Xv, Yv) we get (3) and (4).

$$(1) \Rightarrow Xv = \left(\frac{Yv - y_1}{m_1}\right) + x_1 \tag{3}$$

$$(2) \Rightarrow Xv = \left(\frac{Yv - y_3}{m_2}\right) + x_3 \tag{4}$$

Two unknowns and two equations, viz. (3) and (4), solving for which we get the value of the coordinates (Xv, Yv).

$$Xv = \frac{m_1x_1 - m_2x_3 - y_1 + y_3}{m_1 - m_2} \tag{5}$$

$$Yv = m_1Xv - m_1x_1 + y_1 \tag{6}$$

There are several methods found in the literature to automatically detect vanishing points [20, 23]. Although Hough Transform based methods are found to be better, we use manual vanishing point detection scheme. This is mainly for the two reasons. (1) Our aim in this paper is to introduce about the camera calibration technique and it is not all about finding vanishing point only. Our work extends mainly after finding the vanishing points by exploiting other geometric cues like, picture plane, horizon line, ground line and the station point. (2) Manual vanishing point detection technique

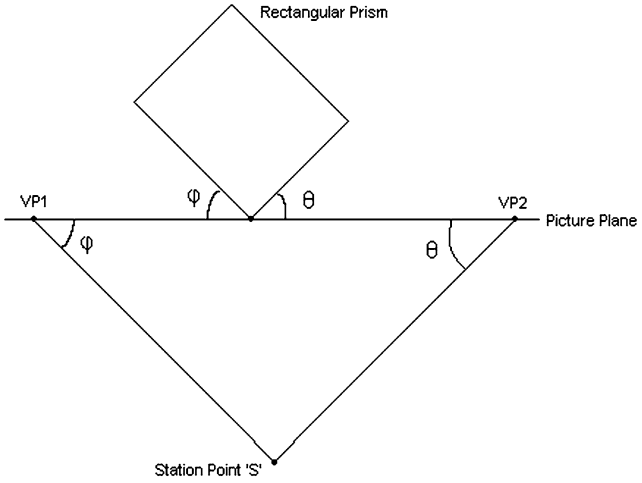

Fig. 2 Depiction of station point from the top view

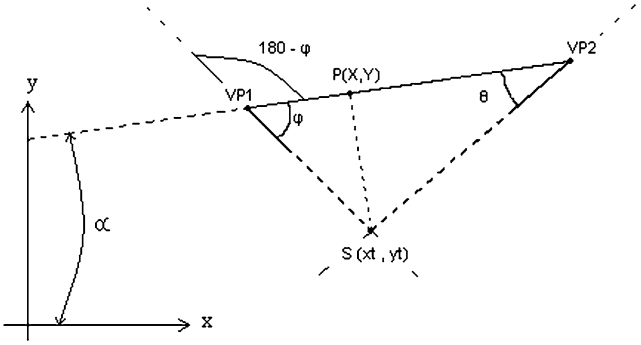

Fig. 3 Points depicted on the top view and their notations

requires very less calculation time than any other method found in the literature.

2.2 Framework for Station Point Detection

Station point is the eye/camera position point. Center of focus [27] is the optical center of the lens used in the camera and it is the point in the camera lens where there is no refraction of light occurring when light is incident on the lens. This point at which the perpendicular light ray is incident pass straight and impinges on the retina of the camera perpendicularly is called the center of focus of the camera on the image. This is found out as discussed in Sect. 4. Objects beyond the picture plane are oriented in some angles. i.e. the faces of the rectangular prism close to the picture plane makes angle θ and φ as shown in Fig. 2. The angular orientation of the calibration object to 45°, what we speak in the later sections is the angles of θ and φ. The point $S(x_t, y_t)$ is fixed up based on (16) and (17), and is the station point. Station point S is the position of the camera focusing towards the picture plane. This is the bird's eye view or the top view of the entire setup. That's the reason the plane (picture plane) appears as a straight line and not as a plane. This is depicted in Fig. 2. To arrive at (16) and (17) for the coordinates of the station point, we come across the following relations.

(u_1, v_1) and (u_2, v_2) are the coordinates of the points V_{P1} and V_{P2} respectively. m is the slope of the line joining these two points V_{P1} and V_{P2}, i.e.

$$m = \tan\alpha = \left(\frac{v_2 - v_1}{u_2 - u_1}\right) \tag{7}$$

$$\alpha = \tan^{-1}\left(\frac{v_2 - v_1}{u_2 - u_1}\right) \tag{8}$$

The images acquired have their x and y coordinates on the picture plane. If there is a rotation along the z axis, that is if the camera has a roll [21, 22], then the horizon line formed doesn't appear parallel to the image coordinates. Hence to make the experimentation roll invariant, we introduce an angle α to generalize the case. Although pan and tilt [21, 22] of the camera has no importance in our experiment. Tilt of the camera introduces the third vanishing point from the calibration object and pan takes the calibration object out of focus from the camera. We are strictly using images with two vanishing points only for our experimentation.

Slope of the line and subsequently the equation of that line having an angle $(180 - \varphi)$ with the line joining two points V_{P1} and V_{P2} and passing through a point V_{P1} (u_1, v_1) on that line as seen in Fig. 3 is given by

$$m_1 = \tan[(180 - \varphi) + \alpha] \tag{9}$$

$$(y - v_1) = m_1(x - u_1) \tag{10}$$

where

$$\tan\alpha = \left(\frac{v_2 - v_1}{u_2 - u_1}\right) \tag{11}$$

Similarly the equation of line passing through (u_2, v_2) with an inclination of θ to the line joining the points V_{P1} and V_{P2} as shown in Fig. 3 is given by (12),

$$(y - v_2) = m_2(x - u_2) \tag{12}$$

$$\Rightarrow\ m_2 = \tan[\theta + \alpha] \tag{13}$$

These lines in (10) and (12) are nonparallel as they are having different inclinations each. They definitely would meet at some point (x_t, y_t) if they are extended on either ends. That is, only at the point at which it intersects satisfies both (10) and (12). Rearranging these equations after substituting (x_t, y_t) we get

$$(10)\ \Rightarrow x_t = \left(\frac{y_t - v_1}{m_1}\right) + u_1 \tag{14}$$

$$(12)\ \Rightarrow x_t = \left(\frac{y_t - v_2}{m_2}\right) + u_2 \tag{15}$$

Two unknowns (x_t, y_t) and two equations, viz. (14) and (15), solving for which we get the value of the coordinates and it is the coordinates of the point S.

$$x_t = \frac{[(v_2 + m_1u_1) - (m_2u_2 + v_1)]}{(m_1 - m_2)} \tag{16}$$

$$y_t = m_1\left[\frac{(v_2 + m_1u_1) - (m_2u_2 + v_1)}{(m_1 - m_2)}\right] - m_1u_1 + v_1 \tag{17}$$

We consider the cases of only 2 vanishing points during image acquisition and thus we see only V_{P1} and V_{P2} as the two points in the image.

2.3 Framework for the Focal Length Determination

Focal length of the camera is the shortest distance from the station point to the picture plane. That is the distance from the points P to S, as shown in Fig. 3. To obtain the focal length, the following relations are derived.

Vector property of orthogonality is given by,

$$aa^1 + bb^1 = 0 \tag{18}$$

where (a, b) and (a^1, b^1) are the directional ratios of $\overrightarrow{V_{P1}V_{P2}}$ and $\overrightarrow{PS}$ as shown in Fig. 3, i.e.

$$(a, b) = [(u_2 - u_1), (v_2 - v_1)] \tag{19}$$

$$(a^1, b^1) = [(x_t - X), (y_t - Y)] \tag{20}$$

$$P(X, Y) \Rightarrow P(u_1 + rl, v_1 + rm) \tag{21}$$

The directional cosines (l, m) of $\overrightarrow{V_{P1}V_{P2}}$ is given by

$$(l, m) = \left(\frac{a}{\sqrt{a^2 + b^2}}, \frac{b}{\sqrt{a^2 + b^2}}\right) \tag{22}$$

Solving equation (18), using (19–22), we get the only unknown r. This is the radius vector

$$r = \frac{a(x_t - u_1) + b(y_t - v_1)}{al + bm} \tag{23}$$

Substituting (22) and (23) into (21), we get values for X and Y at point P. Using the distance formula for points $P(X, Y)$ to $S(x_t, y_t)$ we obtain the distance, i.e. the focal length.

$$|\overrightarrow{PS}| = \sqrt{(x_t - X)^2 + (y_t - Y)^2} \tag{24}$$

3 Experimental Setup and Basic Conventions

The following setup is considered to be taken care of in order to carry out our experimentation and analysis.

1. Images of rectangular prisms are opted as calibration objects for the camera calibration.
2. The calibration objects are aligned during image acquisition so that the image yields two vanishing points for this experiment. These two vanishing points when joined by a straight line, we call the line as horizon line which acts as the eye height from the ground level. The horizon line always passes through the center of vision [17]. Ultimately it is required to find out this point on the horizon line.
3. The calibration object's orientation to the picture plane is noted down. That is the faces of the rectangular prism facing the camera make certain angle to the picture plane. This angle is supposed to be known in order to proceed with the experimentation.
4. The picture plane [15] is also called as the image plane when considered in terms of image. What is seen in Fig. 1 is the front view and hence it is referred to as image plane, but when the same is viewed from top, the plane appears to be a line. This is as seen in Figs. 2 and 3. Here it is referred to as picture plane. But both the terms are used interchangeably in this paper.

With the above settings, the estimation of the camera calibration is analytically calculated in the manner explained in the section that follows.

4 Calibration Algorithm

The previous section gives the necessary setup of the calibration object required for the image acquisition. The image acquired from the setup (single image) is processed with the procedure as given below to find out the focal length and the camera center.

If the ordinate values of the image coordinate points are not changed to the regular convention of the Cartesian coordinate system the vanishing points detected would be based on the image coordinate system and the calculations made with the formulae derived in the regular convention. This results in erroneous results. Thus to give uniformity and to avoid confusion in calculations and substitutions, the image is brought into the conventional Cartesian coordinate system before any calculations could actually be made.

1. Pixel representation of an image is considered with the matrix convention of reading the index of any coordinates. Where as in the regular convention of the coordinate system the abscissa with increasing values from left to right and ordinate values increasing from bottom to top is considered. Since both the indexing are in opposite direction along the y-axis, it is required to bring the image plane into the regular convention before further calculations. For this, (r, c) being the point of consideration in an image of size (h, w) should have $(h - r, c)$ in the new space and there on $(h - r, c)$ shall be considered instead of (r, c).

Table 1a Results of focal lengths for different distance levels and angles orientation of the prism for images from Sony Handycam

Distance	Angles								Mean	Median	Mode
	10	20	30	40	50	60	70	80			
20	907	699	730	717	736	726	697	681	736.625	721.5	691.25
25	891	761	728	721	739	743	698	658	742.375	733.5	715.75
30	988	746	723	719	743	703	689	725	754.5	724	663
35	853	727	703	721	737	756	773	684	744.25	732	707.5
40	734	671	699	709	726	710	758	678	710.625	709.5	707.25
45	630	653	670	712	732	706	757	682	692.75	694	696.5
50	692	689	726	721	709	761	784	691	721.625	715	701.75
55	612	706	697	713	733	706	784	789	717.5	709.5	693.5
60	691	733	723	723	736	720	781	859	745.75	728	692.5
65	850	663	688	727	745	766	797	721	744.625	736	718.75
70	716	718	739	704	738	722	773	688	724.75	720	710.5
75	680	748	696	706	719	759	779	791	734.75	733.5	731
80	626	715	668	741	741	711	863	764	728.625	728	726.75
Mean	759.2308	709.9231	706.9231	718	733.3846	729.9231	764.0769	723.9231			
Median	716	715	703	719	736	722	773	691		721	
Mode	629.5385	725.1538	695.1538	721	741.2308	706.1538	790.8462	625.1538			

2. To each set of parallel edges, the vanishing point is determined as explained in Sect. 2.1.
3. Step 2 is repeated until all the vanishing points are detected. (In our case, based on the experimental setup, we have selected images which yield only two vanishing points.) The line joining these two vanishing points is called the 'Horizon Line'.
4. A line is drawn parallel to the horizon line, and this is called as the 'Picture Plane'. This plane appears as a line, as it is viewed from the top [17].
5. The station point is fixed up as explained in Sect. 2.2.
6. The focal length is the perpendicular dropped to the picture plane from the station point. This is calculated as explained in Sect. 2.3.
7. The locus of the line joining points P and S when extended on either ends, cuts the horizon line at the point C. This point is the actual center of focus or the optical center of the camera. This is calculated with (5) and (6) as shown in Sect. 2.1 but replacing points (x_1, y_1) and (x_2, y_2) with $P(X, Y)$ and $S(x_t, y_t)$ respectively and (x_3, y_3) and (x_4, y_4) with $V_{P1}(u_1, v_1)$ and $V_{P2}(u_2, v_2)$ to obtain $C(x, y)$ instead of (Xv, Yv).

5 Experimentation and Results

The proposed algorithm has been tested on real data and compared to Zhang's method of camera calibration. We adopt a two step experimental approach, viz.,

1. Selecting 45° orientation of the calibration object to be optimal position.
2. Camera calibration by our method and comparison of Zhang's method with our method.

5.1 Step 1

In this section, we show that 45° orientation of the calibration object to the camera face gives good consistent results of the focal lengths with very less standard deviation from the averaged central result.

A calibrated sliding table is selected for this experiment. The table contains marks with intervals of one centimeter each upon which the slider moves. At steps of 5 centimeters each distance levels are fixed and with the angular orientation of 10° each starting from 10° to 80°, series 1 to series 8 are fixed. At all levels and series, images are captured. All these images are subjected to the algorithm mentioned in Sect. 4. This process is repeated for two different cameras, viz., Sony Handycam and Sony Cybershot. With the help of the above derived formulation, the focal length are calculated for each combination of distance levels and series and the results obtained are as tabulated in Tables 1a and 1b. Measures of central tendencies [19] are applied on these to find the central value of the focal length for these cameras. The results for the measures of central tendencies are also depicted in these tables. Mean, median and mode are calculated for each column and each row. Median for all the obtained means, medians and modes are calculated to come to a standard single central value. This value is shown at

Table 1b Results of focal lengths for different distance levels and angles orientation of the prism for images from Sony Cybershot

Distance	Angles								Mean	Median	Mode
	10	20	30	40	50	60	70	80			
0	1745	2066	2184	2252	2270	2179	2054	2117	2108.375	2148	2227.25
5	1698	2135	2191	2236	2252	2231	2056	2001	2100	2163	2289
10	1997	2131	2194	2266	2261	2251	2169	2063	2166.5	2181.5	2211.5
15	1968	2240	2251	2297	2290	2268	2153	2114	2197.625	2245.5	2341.25
20	2013	2241	2294	2294	2304	2287	2224	2166	2227.875	2264	2336.25
25	1550	2240	2282	2279	2342	2295	2276	2320	2198	2280.5	2445.5
30	2022	2158	2250	2299	2279	2318	2284	2571	2272.625	2281.5	2299.25
35	2124	2138	2259	2343	2271	2336	2276	2793	2317.5	2273.5	2185.5
40	2231	2204	2341	2314	2284	2376	2384	2614	2343.5	2327.5	2295.5
45	2200	2270	2159	2284	2333	2347	2675	2279	2318.375	2281.5	2207.75
50	2010	1968	2275	2276	2346	2397	2560	3049	2360.125	2311	2212.75
Mean	1959.818	2162.818	2243.636	2285.455	2293.818	2298.636	2282.818	2371.545			
Median	2010	2158	2251	2284	2284	2295	2276	2279		2272.625	
Mode	2110.364	2148.364	2265.727	2281.091	2264.364	2287.727	2262.364	2093.909			

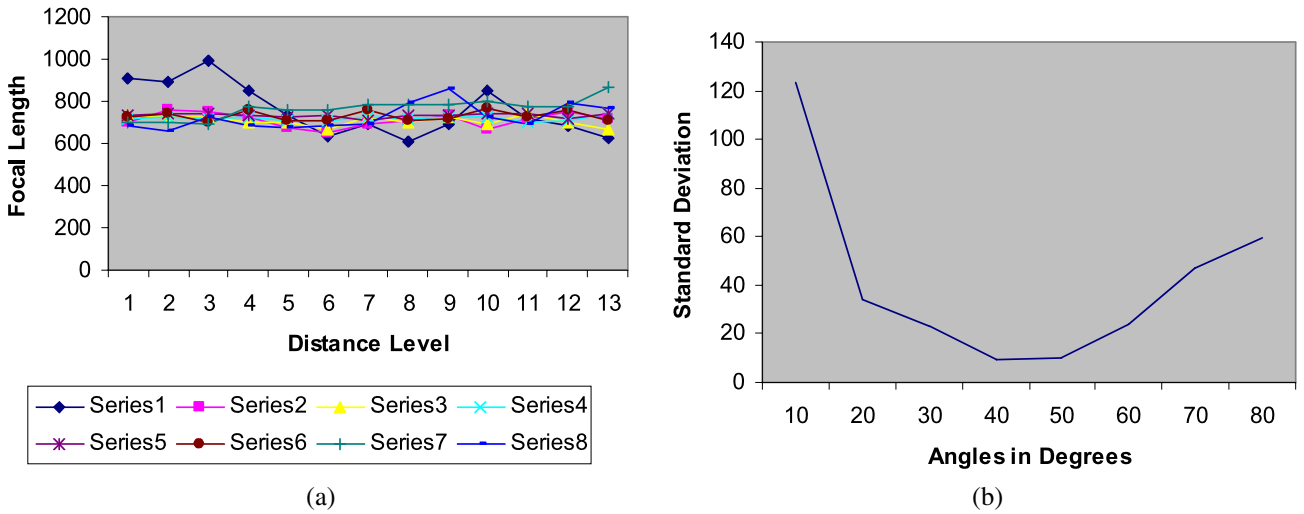

(a) (b)

Fig. 4 **a** Focal length variation for different distance levels for the values given in Table 1a for its respective camera. **b** Standard deviation of the mean values of the focal length for values in Table 1a at different angle orientations

the intersecting row and column of the medians. Figures 4a and 5a depict the graphical representation of variation of focal length for each series along different levels. The standard deviation of variations in the values of focal lengths obtained for all the series, when plotted for tabulation in Tables 1a and 1b, a bath tub curve is obtained. This is shown in Figs. 4b and 5b for their corresponding cameras. From Figs. 4b and 5b, it is evident that there is very less deviation of values of focal lengths from the standard central value at angles between the range of 40° to 50°. Thus we consider 45° orientation of the calibration object for our calibration experiment as a standard value. The future experimentation is required for calculations to compare the results with Zhang's method.

5.2 Step 2

A rectangular prism with one face having a checker board is considered for the following experiments. The rectangular prism acts as the calibration object for our method of camera calibration and the checker board pattern acts as the calibration object for the Zhang's method of camera calibration. These two experiments are carried out and the results are tabulated in Table 3. A series of 20 images each with the cameras mentioned in Table 2 are captured with differ-

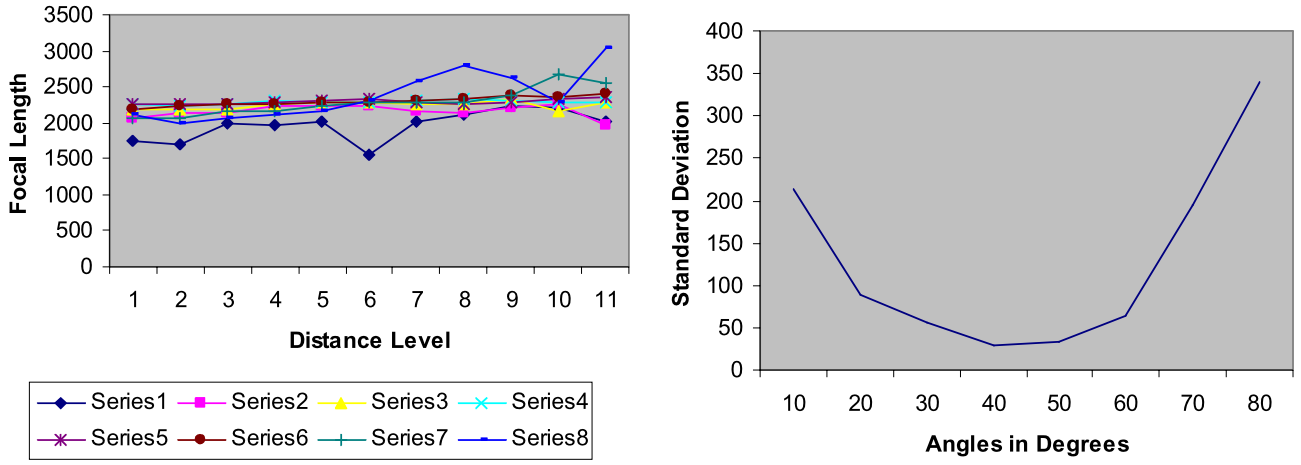

(a) (b)

Fig. 5 **a** Focal length variation for different distance levels for the values given in Table 1b for its respective camera. **b** Standard deviation of the mean values of the focal length for values in Table 1b at different angle orientations

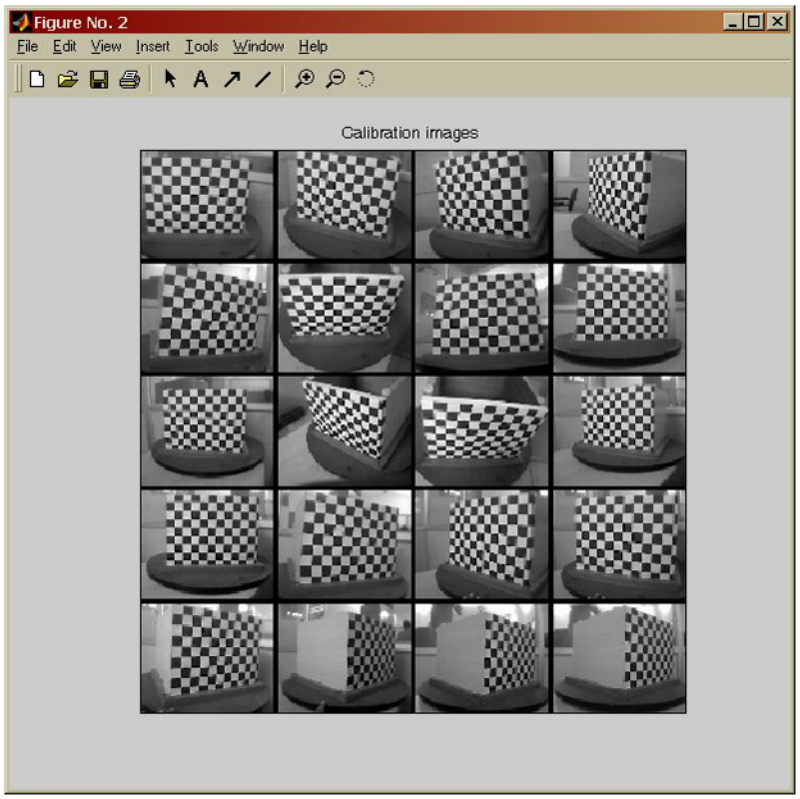

Fig. 6 Zhang's method input of 20 images taken from 6610 camera

Table 2 Cameras used and their picture resolutions

Type	Resolution
Nokia 6610i camera phone	352 × 288
Nokia 9500 communicator Phone	640 × 480
Sony Handycam HC40E	640 x 480

ent orientations and directions. These sets of images are as shown in Figs. 6 through 8. This acts as input to the Zhang's method. Results are found out and are tabulated as shown in Table 3b for Zhang's method.

Certain images among the set of 20 images selected for the Zhang's method satisfies the condition for our method. Those images are shown in Figs. 9 through 14. These images act as input images for our method. Results are found out

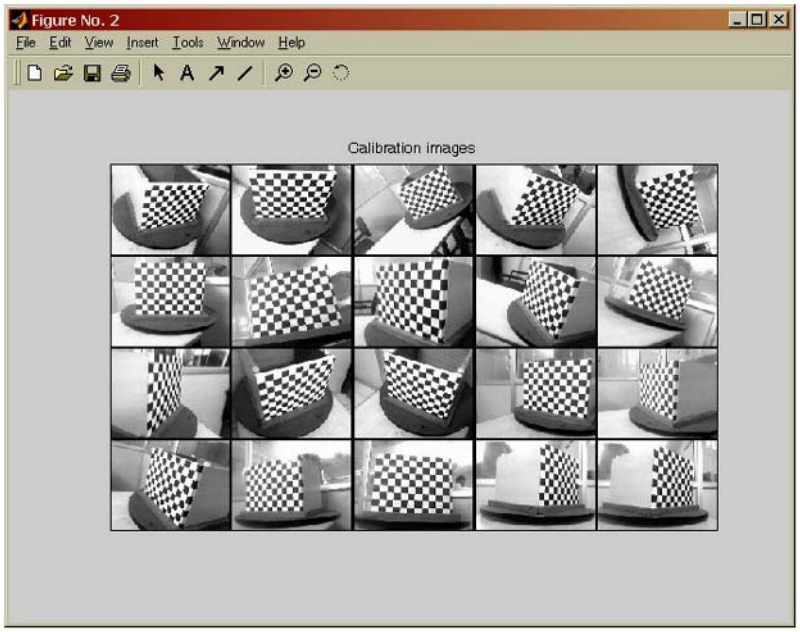

Fig. 7 Zhang's method input of 20 images taken from 9500 camera

Fig. 8 Zhang's method input of 20 images taken from HC40E camera

Table 3a Results of our method

Image from	Our method (for single image)		
	Focal length	cc(x)	cc(y)
6610 Image 1	372.16	166.55	131.21
6610 Image 2	371.83	165.32	130.98
9500 Image 1	675.63	304.25	225.42
9500 Image 2	675.9	311.76	228.21
HC40E Image 1	719.13	314.09	223.17
HC40E Image 2	720.06	314.67	222.82

based on the calibration algorithm stated in Sect. 4 and the results of all these images are individually calculated. They are as shown here in Table 3a.

Table 3b Results of Zhang's method

Images from	Zhang's method (for 20 images)		
	Focal length (range)	cc(x)	cc(y)
6610	[371.6244 371.29673]	166.8477	131.2704
9500	[675.14273 676.62074]	308.8402	226.3764
HC40E	[718.98027 722.92162]	311.7551	220.1777

From the results it is evident that the results we get from both the methods have almost similar results. But the point to be noted are, in our method the initial knowledge of the orientation of the rectangular prism is to be known unlike in Zhang's method of viewing plane from unknown orientations. But to obtain these similar results from the latter,

Fig. 9 Image 1 captured from Nokia 6610 camera

Fig. 10 Image 2 captured from Nokia 6610 camera

Fig. 11 Image 1 captured from Nokia 9500 camera

Fig. 12 Image 2 captured from Nokia 9500 camera

Fig. 13 Image 1 captured from HC40E camera

Fig. 14 Image 2 captured from HC40E camera

multiple images are required whereas in our method a single image is sufficient. The process is iterative in the case of Zhang's method and the values converge to the desired result over multiple iterations. This consumes more time for calculation. Whereas in our case, the calculations are analytical and straightforward (non iterative) and hence takes lesser time for computation. The major recede of Zhang's method is that, it requires crusaded manual interaction in the process of selecting the corner points of the checker board. In our method, this process is considerably reduced as the image considered for calibration is one only and the points to be selected are just 6 instead of 80 as in the case of Zhang's method for 20 images.

6 Conclusion

The paper presents a method for camera calibration, based on the use of two vanishing points. Although the results obtained with the method proposed in this paper are almost the same as the results obtained using the Zhang's method, this method has the advantage of being analytical and straightforward, non iterative. Therefore it consumes less time. Other advantages of the proposed is that it requires only one image, and the manual selection of only six points; in contrast, Zhang's method requires several images, selecting manually several points (corners of the checker board) for each image, which are used in the iterative solution.

The main disadvantage is that the proposed method requires a specific setup to work properly; that is, the orientation of the rectangular prism used for calibration has to be known, unlike the Zhang's method, which uses images of the plane in unknown orientations.

References

1. Slama, C.C.: Manual of Photogrammetry, 4th edn. American Society of Photogrammetry, Falls Church (1980)
2. Tsai, R.Y.: A versatile camera calibration technique for high-accuracy 3D machine vision metrology using off-the-shelf TV cameras and lenses. IEEE Journal of Robotics and Automation **3**(4), 323–344 (1987)
3. Abdel-Aziz, Y.I., Karara, H.M.: Direct linear transformation into object space coordinates in close-range photogrammetry. In: Proc. Symposium on Close-Range Photogrammetry, pp. 1–18. Urbana, Illinois (1971)
4. Caprile, B., Torre, V.: Using vanishing points for camera calibration. Int. J. Comput. Vision **4**, 127–140 (1990)
5. Beardley, P., Murray, D., Zisserman, A.: Camera calibration using multiple images. In: Proc. Eur. Conf. Comput. Vision, pp. 312–320 (1992)
6. Echigo, T.: A camera calibration technique using three sets of parallel lines. Mach. Vis. Appl. **3** (1990)
7. Chen, W., Jiang, B.: 3-D camera calibration using vanishing points concept. Pattern Recogn. **24**(1) (1991)
8. Kanatani, K.: Geometric Computation for Machine Vision. Oxford University Press, London (1993). ISBN 0-19-856385-X
9. Wang, L.-L., Tsai, W.-H.: Camera calibration by vanishing lines for 3-D computer vision. IEEE Trans. Pattern Anal. Mach. Intell. **13**(4), 370–376 (1991)
10. Brillault, B., O'Mahony: New method for vanishing point detection. CVGIP: Image Underst. **54**(2), 289–300 (1991)
11. Li, M.: Camera calibration of the KTH head-eye system. In: ECCV94, pp. A:543–554 (1994)
12. Lobo, J., Dias, J.: Fusing of image and inertial sensing of camera calibration. In: Proc. International Conf. Multisensor Fusion and Integration for Intelligent Systems, pp. 103–108, Aug. 2001
13. Willson, R.G., Shafer, S.A.: What is the center of the image? In: Conference on Computer Vision and Pattern Recognition, pp. 670–671 (1993)
14. Benosman, R., Maniere, T., Devras, J.: Panoramic sensor calibration using computational projective geometry. In: Proc. of the 1997 IEEE International Conference on Robotics and Automation, Albuquerque, New Mexico, April 1997
15. Murali, S., Avinash, N.: Estimation of depth information from a single view in an image. In: ICVGIP, pp. 202–209 (2004)
16. Collins, R.T., Weiss, R.: An efficient and accurate method for computing vanishing points. In: Proc. Topical Meeting of the Optical Society of America on Image Understanding, pp. 92–94 (1989)
17. Dobrovolny, J.S., O'Bryant, D.C.: Graphics for Engineers, 2nd edn. Wiley, New York (1984). ISBN 0-471-87124-9
18. Zhang, Z.: A flexible new technique for camera calibration. IEEE Trans. Pattern Anal. Mach. Intell. **22**(11), 1330–1334 (2000)
19. Garret, H.E.: Statistics in Psychology and Education. Vakils, Feffer & Simons Pvt. Ltd., Bombay (1973). Chap. 2: Measures of Central Tendency, pp. 27–41
20. Mavaddat, N.: Research proposal. Available at www.csse.uwa.edu.au/~navid/proposal.pdf, April 2002
21. Fjeld, M., Ironmonger, N., Voorhorst, F., Bichsel, M., Rauterberg, M.: Camera control in a planar, graspable interface. In: 17th IASTED International Conference on Applied Informatics (AI'99), pp. 242–245 (1999)
22. Jakobsen, O.C., Johnson, E.N.: Control architecture for a UAV-Mounted Pan/Tilt/Roll Camera Gimbal. In: Proc. AIAA Guidance, Infotech@Aerospace Arlington, Virginia, Sept. 2005
23. Avinash, N., Murali, S.: A voting scheme for inverse hough transform based vanishing point determination. In: International Conference on Cognition and Recognition, Mysore, India, Dec. 2005
24. Vezhnevets, V.: At the Department of Graphics and Media Lab, MSU. Available at http://graphics.cs.msu.su/en/research/calibration/index.html
25. Bouguet, J.-Y.: Camera Calibration Toolbox for Matlab®. http://www.vision.caltech.edu/bouguetj/calib_doc/
26. Intel OpenCV Computer Vision Library (C++). http://www.intel.com/research/mrl/research/opencv/
27. Douglas, A., Kerr, P.E.: The Proper Pivot Point for Panoramic Photography, Issue 2. The Pumpkin, New York (2005)

N. Avinash received the Bachelors degree in Mechanical Engineering in 2001 and the Masters in Computer Cognition Technology in 2003, from the University of Mysore, Mysore, India. He is currently working towards the Ph.D. degree in the Department of Information Science and Engineering, P.E.T. Research Centre, P.E.S. College of Engineering, Mandya, affiliated to University of Mysore. His research interests are in the area of Computer Vision and Image Processing, Document Image Processing and Robotics.

S. Murali received the Bachelors degree in Electronics and Communication Engineering in 1988, Masters in Computer Technology in 1994 and the Ph.D. degree in 2002 in Document Image Processing from the University of Mysore, India. From 1988 to 1994 he was a Lecturer and in 1994 he joined the P.E.S. College of Engineering, Mandya, India, affiliated to the University of Mysore ever since he is serving as an Assistant Professor and now Professor (since 2003). He is the author of more than 35 contributions to international conferences and journals. His research interests are in the area of Computer Vision, Data Mining, Document Image Processing, Medical Imaging. He has executed 5 funded projects from the UGC and AICTE in India.